Environmental Science & Technology

Article

Cite This: Environ. Sci. Technol. 2018, 52, 13501−13510

pubs.acs.org/est

Changes in microRNA−mRNA Signatures Agree with Morphological, Physiological, and Behavioral Changes in Larval Mahi-Mahi Treated with *Deepwater Horizon* Oil

Elvis Genbo Xu,[*,†,∥] Jason T. Magnuson,[‡] Graciel Diamante,[†] Edward Mager,[‡] Christina Pasparakis,[§] Martin Grosell,[§] Aaron P. Roberts,[‡] and Daniel Schlenk[*,†]

[†]Department of Environmental Sciences, University of California, Riverside, California 92521, United States

[‡]Department of Biological Sciences & Advanced Environmental Research Institute, University of North Texas in Denton, Denton, Texas 76203, United States

[§]Department of Marine Biology and Ecology, RSMAS, University of Miami, Miami, Florida 33149, United States

Supporting Information

ABSTRACT: In this study, we performed a systematic evaluation of global microRNA−mRNA interactions associated with the developmental toxicity of *Deepwater Horizon* oil using a combination of integrated mRNA and microRNA deep sequencing, expression profiling, gene ontology enrichment, and functional predictions by a series of advanced bioinformatic tools. After exposure to water accommodated fraction (WAF) of both weathered slick oil (0.5%, 1%, and 2%) and source oil (0.125%, 0.25%, and 0.5%) from the *Deep Water Horizon* oil spill, four dose-dependent miRNAs were identified, including three up-regulated (miR-23b, miR-34b, and miR-181b) and one down-regulated miRNAs (miR-203a) in mahi-mahi hatchings exposed from 6 h postfertilization (hpf) to 48 hpf. Consistent with morphological, physiological, and behavioral changes, the target genes of these miRNAs were largely involved in the development of the cardiovascular, visual, nervous system and associated toxicity pathways, suggesting that miRNAs play an essential role in regulating the responses to oil exposure. The results obtained from this study improve our understanding of the role of miRNAs and their target genes in relation to dose-dependent oil toxicity and provide the potential of using miRNAs as novel biomarkers in future oil studies.

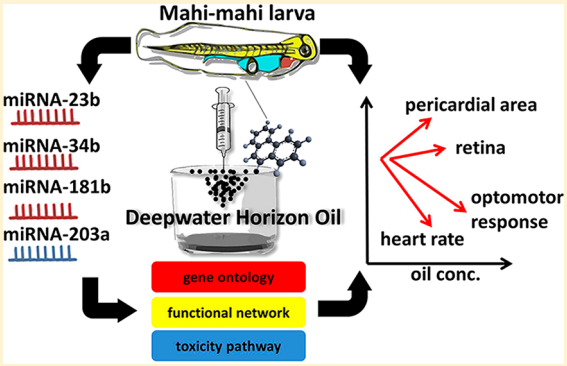

INTRODUCTION

In 2010, the *Deepwater Horizon* (DWH) oil spill released millions of barrels of oil into the Gulf of Mexico,[1] coinciding with peak spawning periods of economically and ecologically important pelagic fishes.[2−4] Measured concentrations of polycyclic aromatic hydrocarbons (PAHs) in the Gulf of Mexico surrounding the spill ranged from below detection to 84.8 μg/L.[5] Some samples were as high as 240 μg/L in the upper subsurface.[6] The composition of PAHs in crude oil can be altered by natural weathering, which can increase the amount of 3- and 4-ring PAHs and increase toxicity to larval fish.[7] Furthermore, PAHs present in DWH crude oil has been related to developmental impairment and mortality in pelagic fishes, such as yellowfin tuna (*Thunnus albacares*), bluefin tuna (*Thunnus maccoyii*), amberjack (*Seriola lalandi*), and mahi-mahi (*Coryphaena hippurus*).[7,8]

Marine pelagic fish develop rapidly, with mahi-mahi hatching within 36−40 h postfertilization (hpf). Early developmental stages are particularly vulnerable to PAH toxicity, with LC_{50} concentrations ranging from 19 μg/L to 146 μg/L total PAHs (TPAHs) during the first 48 h of mahi-mahi development.[9] In combination with UV-radiation, the 96-h LC50 of DWH slick oil can be as low as 0.7 μg/L.[10] Furthermore, pericardial edema, abnormal looping, and reduced contractility of the heart were seen in larval mahi-mahi following exposures to <10 μg/L TPAHs,[11] with swimming performance also impaired in juvenile mahi-mahi following larval exposure to 1.2 μg/L TPAHs.[12] Pathway predictions from global mRNA sequencing indicated cardiac impairment would be the highest impacted biological pathway following exposure, along with reduced photoreceptor-specific functions.[13,14] The mechanisms that altered the regulation of the mRNAs were not explored but it was hypothesized that transcription may be epigenetically modified by microRNAs (miRNAs).

miRNAs are short noncoding RNAs of 18−25 nt that regulate large numbers of mRNAs by directing the RNA-induced silencing complex (RISC) to target mRNAs, and the miRNA−mRNA interactions that occur at the post-transcriptional level can largely influence gene expression.[15] miRNAs

Received: July 27, 2018
Revised: October 23, 2018
Accepted: October 30, 2018
Published: October 30, 2018

DOI: 10.1021/acs.est.8b04169
Environ. Sci. Technol. 2018, 52, 13501−13510

have been shown to regulate diverse biological processes, including cell proliferation, differentiation, and apoptosis in different species.[16−19] Recent mammalian and piscine studies found that PAH exposure can regulate the expression of miRNAs, which influenced mRNA expression and development.[20−23] In our previous studies, we found the expression of mRNA and miRNAs were dependent on the developmental stages of fish post DWH crude oil exposure with more differentially expressed (DE) miRNA at later larval stages.[22,24] In light of their critical role in early development, we hypothesized that miRNAs might regulate dose-dependent transcriptional responses of larval fish to DWH crude oil. In this study, we generated comprehensive miRNA and mRNA expression profiles, and evaluated miRNA−mRNA interactions associated with DWH oil exposure of different concentrations and their influence on subsequent morphological, physiological, and visual-mediated behavioral impairments in larval fish.

MATERIALS AND METHODS

Animals and DWH Oil Exposure. Mahi-mahi broodstock was caught off the coast of South Florida using hook and line angling techniques and then directly transferred to the University of Miami Experimental Hatchery (UMEH). Broodstock were acclimated in 80 m^3 fiberglass maturation tanks equipped with recirculating and temperature-controlled water. All embryos used in the experiments described here were collected within 2−10 h following a volitional (noninduced) spawn using standard UMEH methods.[25] Two sources of crude oil from the DWH spill that varied with respect to weathering state were obtained from British Petroleum under chain of custody for testing purposes: (1) slick oil collected from surface skimming operations (sample ID: OFS-20100719-Juniper-001 A0091G) and (2) oil from the Massachusetts barge (sample ID: SO-20100815-Mass-001 A0075K) which received oil collected from the subsea containment system positioned directly over the well (referred to herein as slick and source oil, respectively). Preparation of high energy water accommodated fractions (HEWAFs) of two oil types and oil exposures were performed at the University of Miami as outlined previously.[13]

A flowchart of the experimental design is provided in Figure S1 of the Supporting Information (SI). For miRNA−mRNA sequencing and 48-h morphometric analyses, exposures were started at 6 hpf until 48 hpf at three nominal concentrations based on LC_{25} in previous study: 0.5%, 1%, and 2% HEWAF of slick oil or 0.125%, 0.25% and 0.5% HEWAF of source oil. Three replicates were used per concentration with 25 hatched larvae per replicate. Embryos were statically treated in 1L glass beakers. Water quality (i.e., temperature, pH, DO, and salinity) was monitored and is reported in Table S1. Slick and source oil HEWAF exposures were run concurrently using the same batch of embryos and a shared set of controls for both sets of experiments. Embryos were monitored daily and dead embryos were removed. The 48 hpf life stage for RNA analyses was selected based on earlier studies evaluating stage susceptibility to oil toxicity.[13] In a second experiment, 7 to 10 day post hatch (dph) mahi-mahi were assessed daily for histological and behavioral effects following exposure to lower concentrations of slick oil HEWAFs (0.08% and 0.2%) from 6 hpf until 36 hpf. Exposure was stopped at 36 hpf to minimize the potential variations between hatched and unhatched embryos on behaviors, and older larvae were needed to determine an optomotor response comparing to the earlier stage larvae used for mRNA−miRNA sequencing. All animal experiments were performed ethically and in accordance with Institutional Animal Care and Use Committee (IACUC protocol number 15−019) approved by the University of Miami IACUC committee, and the institutional assurance number is A-3224−01.

Water Chemistry Analysis. PAH concentrations were measured by gas chromatography/mass spectrometry−selective ion monitoring (GC/MS-SIM; based on EPA method 8270D) according to Xu et al.[13] Briefly, 250 mL subsamples of diluted HEWAF were collected at the beginning of the treatment (6 hpf) and at the end of the treatment (48 hpf)in an amber bottle for each exposure dilution and stored at 4 °C until shipped to ALS Environmental (Kelso, WA, U.S.A.) for PAH analysis.

Physiological, Morphological, and Histological Measurements. Following treatments larvae were mounted on a Nikon SMZ800 stereomicroscope with images collected at 48 hpf for pericardial area, eye area, and heart rate using iMovie software on a MacBook laptop. Twenty larval mahi-mahi (7 to 10 dph) per treatment per dph were assessed in the behavioral assay. This stage was selected based on logistics of size and movement for the behavioral assays below. Ten random individuals per treatment per dph were fixed in Bouin's solution and later assessed for total length and eye measurements. Larvae were subsequently dehydrated in ethanol solutions and embedded in paraffin. A microtome was used to make 5 μm sections of the left eye, with sections adhered to poly-L-lysine-coated slides and stained with hematoxylin and eosin. The retina, lens, ganglion, inner plexiform layer, inner nuclear layer, outer plexiform layer, outer nuclear layer, photoreceptor layer, and the pigmented epithelial layer diameters were imaged on an Axio imager A1 Zeiss compound microscope (200× magnification), with images analyzed using ImageJ (version 1.47).

Behavioral Assessment−Optomotor Response (OMR). An OMR was assessed in 7 to 10 dph mahi-mahi larvae. An OMR was determined by the ability of a larva to following a rotating black or white vertical stripe in both clockwise and counterclockwise directions. The stripes subtended a 22° angle from the center of the tube to the rotating drum. The fish were transferred to the chamber using a wide-mouth transfer pipet and allowed to acclimate to the chamber for 1 min, as a longer duration of time did not exhibit a change in normal swimming behavior. The cylinder in which the stripes adhered were driven by a 100 rpm (rotations per minute) motor. An attached potentiometer was used to assess rotational speed, with speeds ranging from 7 to 30 rpm. The speed of the stripes remained at 7 rpm until the larvae were able to follow the rotating stripes and then increased incrementally until the larvae were unable to follow the rotating stripes, at which point the maximum rotational speed was recorded.

mRNA Sequencing, Assembly, and Annotation. A detailed method of mRNA sequencing is presented in Xu et al.[26] The surviving 48 hpf larvae from each replicate were pooled and RNA was isolated and purified with RNeasy Mini Kit (Qiagen, Valencia, California). 200 ng of total RNA was used to prepare RNA-Seq libraries using the NEBNext Ultra II Directional RNA Library Prep Kit for Illumina following the protocol described by the manufacturer (Ipswich, MA). Single Read 1 × 75 sequencing was performed on Illumina NextSEQ v2 with each individual sample sequenced to a minimum depth of ~50 million reads. Data were subjected to Illumina quality control (QC) procedures (>85% of the data yielded a Phred score of 30). The read data were deposited in the NCBI database (Accession Number: GSE116639).

DOI: 10.1021/acs.est.8b04169
Environ. Sci. Technol. 2018, 52, 13501−13510

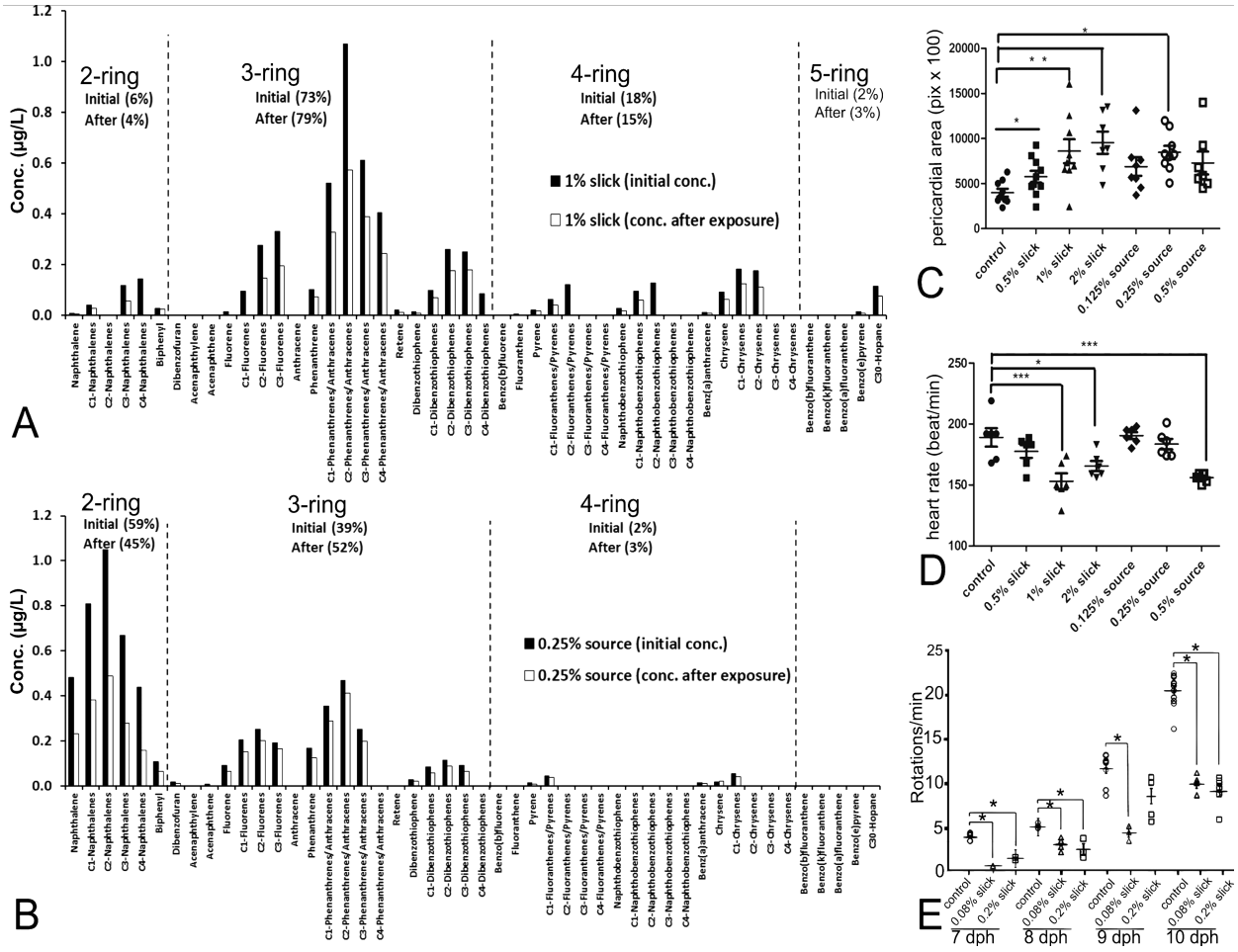

Figure 1. Percent composition for 50 PAH analytes as determined by GC−MS for HEWAF of 1% slick (A) and 0.25% source DWH oil (B). Assessment of pericardial area (C), heart rate (D) in 48 hpf mahi-mahi exposed to slick or source oil HEWAF. Average rotations/min in 7, 8, 9, and 10 day post hatch (dph) mahi-mahi exposed to 0.08% and 0.2% slick oil HEWAF (E). Data are presented as mean ± SEM (n = 8 for Figure 1c and 1d, and n = 20 for Figure 1e). * indicate significant differences between control and oil exposed larvae (one-way ANOVA, Bonferroni post hoc).

Raw sequences were trimmed off Illumina adapter sequences and filtered out sequences that did not meet the quality thresholds using Trimmomatic (version 0.33). All reads were pooled and assembled de novo using Trinity (version 2.2.0) with k-mer length set at 25. Subsequently, the high-quality reads were mapped to the Trinity assembled *de novo* mahi-mahi transcriptome to estimate the transcript/Unigene abundance using RSEM (RNA-Seq by Expectation-Maximization) (version 1.2.21) with the default aligner Bowtie (version 1.1.1). The expression level of each transcript/Unigene was measured with FPKM (fragments per kilobase per million reads). Statistical differences in gene expression levels between mahi-mahi larvae exposed to DWH oil and controls were calculated using DEseq2. Genes were considered differentially expressed when false discovery rate (FDR) < 0.01 (Benjamini−Hochberg correction). Trinotate (2.0.2) was used for functional annotation, including homology search to known sequence data.

Gene Ontology and Ingenuity Pathway Analyses. The sorted transcript lists were mapped to human orthologs to generate HGNC (HUGO Gene Nomenclature Committee) gene symbols for downstream gene ontology (GO) term analysis, using DAVID Bioinformatics Resources 6.8 (*Danio rerio* as reference)and ToppGene Suite. GO terms for biological process were considered significantly enriched when $p < 0.05$. Ingenuity Pathway Analyses (IPA) (Ingenuity Systems Inc., Redwood City, CA, USA) was used to compare at different oil types and concentration conditions to identify similarities and differences in canonical pathways and toxicity functions (IPA-Comparison analysis). Fisher's exact test was used to calculate a p-value determining the probability that the association between the genes in the data set and the IPA-Tox pathways as opposed to this occurring by chance alone.

miRNA Isolation, Sequencing, and Annotation. The miRNA sequencing and annotation followed Diamante et al.[22] with minor modifications. Briefly, miRNAs were isolated from the same pooled 48 hpf larval samples as used for mRNA extraction above, using the miRNeasy mini kit from Qiagen (Valencia, CA). miRNA libraries were made using the New England Biolabs NEBNext Multiplex Small RNA Sample Prep kit (Ipswich, MA) following the manufacturer's protocol. The size distribution and concentration of the libraries were determined using the Agilent High Sensitivity DNA Assay Chip (Santa Clara, CA). Single Read 1 × 75 sequencing was performed on an Illumina NextSEQ v2. The read data were deposited in the NCBI database (Accession Number: GSE116711).

The quality of the raw miRNA sequences was evaluated by FastQC toolkit (Cambridge, U.K.). Adaptor sequences were trimmed off using the FASTX toolkit (Cambridge, U.K.), to obtain a mean Phred score ≥30. Only reads that are longer than

DOI: 10.1021/acs.est.8b04169
Environ. Sci. Technol. 2018, 52, 13501−13510

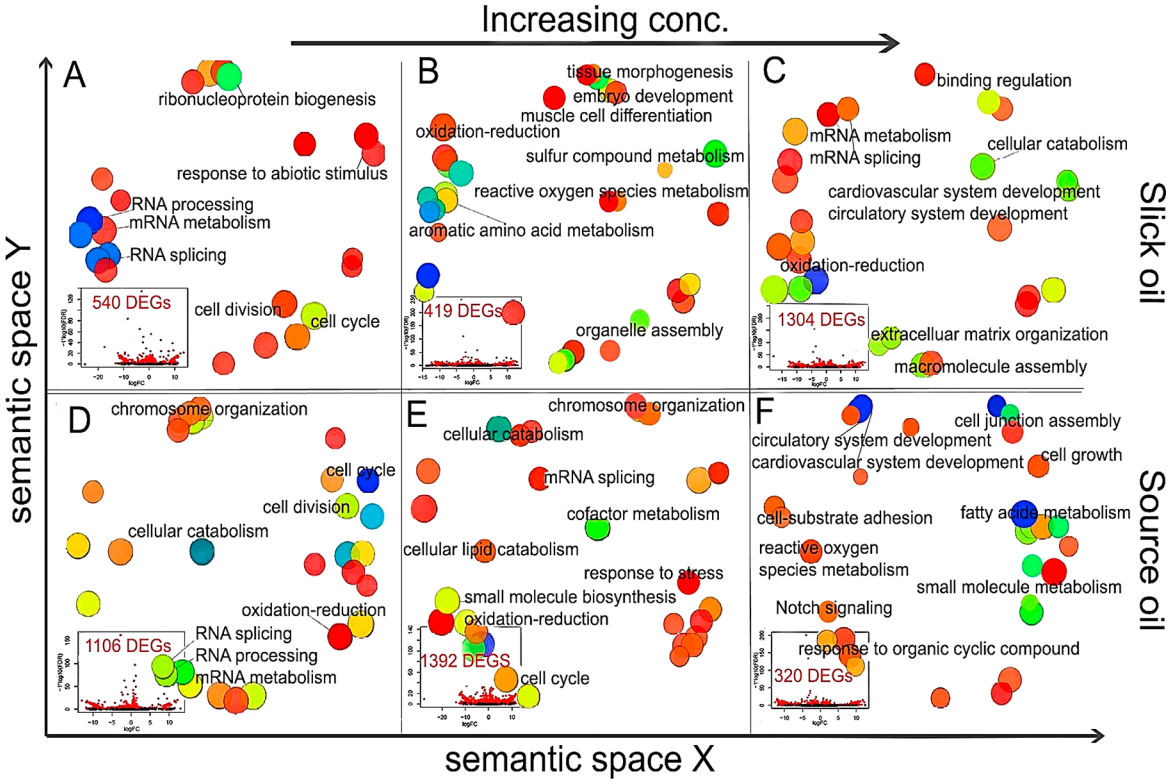

Figure 2. Top enriched biological processes in mahi-mahi exposed to 0.5% (A), 1% (B), 2% (C), of slick or 0.125% (D), 0.25% (E), and 0.5% (F) of source oil HEWAF by ToppGene. The scatterplots show cluster members in a two-dimensional space obtained by applying multidimensional scaling of a matrix of the gene ontology (GO) terms' semantic similarities. The proximity on the plot reflects the semantic similarity. Blue and green circles indicate greater significance than orange and red circles. The size of the circle indicates the GO term frequency in the GO database.

18 bp and shorter than 30 bp were kept for downstream alignment. The processed reads were mapped to the *Fugu rubripes* genome, and both known and novel miRNAs were identified using miRDeep2. Read counts generated from miRDeep2 were used for differential expression analysis using DESeq2. Identified differentially expressed miRNAs and mRNA-seq data from the samples were analyzed using the microRNA Target Filter in IPA to identify experimentally demonstrated miRNA−mRNA relationships and predict the impact of expression changes of miRNA and its target mRNA on biological processes and pathways. A miRNA was considered to be regulatory only if the expression levels of miRNA and its mRNA targets are reversely correlated.

RESULTS

Chemical Composition of Weathered Slick Oil and Source Oil. The concentrations of PAHs in weathered slick oil and source oil were measured before and after oil exposures. The initial and final concentrations of TPAHs in 0.5%, 1%, and 2% slick oil were 3.09 and 1.82 μg/L, 6.25 and 4.07 μg/L, and 13.40 and 11.67 μg/L, respectively (Table S2). The initial and final concentrations of TPAHs in 0.125%, 0.25%, and 0.5% source oil were 9.39 and 5.38 μg/L, 16.37 and 9.82 μg/L, and 36.57 and 27.08 μg/L, respectively (Table S2). A loss of 2-ring PAHs, as well as enrichment of 3-ring and larger PAHs, were observed during weathering processes of source to slick oil. The weathered slick oil predominantly consisted of 3-ring compounds (Figure 1a), while the source oil was comprised predominantly of 2-ring PAHs followed by 3-ring PAHs (Figure 1b), represented largely by the naphthalenes and phenanthrenes/anthracenes, respectively (Table S2).

Morphological and Physiological Measurements. Both slick and source oil increased the mean pericardial area in 48 hpf mahi-mahi larvae. The slick oil treatment significantly increased pericardial area at 0.5%, 1%, and 2% concentrations compared to controls, and this was also significant under 0.25% source oil treatment (Figure 1c). In addition, the 0.5%, 1%, and 2% slick oil and 0.5% source oil treatments significantly decreased heart rate compared to controls (Figure 1d). The size of eyes in larvae was not significantly affected by slick or source oil treatment at 48 hpf (Figure S2). However, larvae at later stages (7−10 dph) exposed to two lower concentrations of slick oil [0.08% (0.67 μg/L TPAHs) and 0.2% (1.14 μg/L TPAHs)] had significantly larger retinas, inner nuclear and ganglion layer diameters than controls (Figure S3).

Behavioral Response. Oil-exposed larvae exhibited a significantly reduced OMR compared to controls (52.5 ± 12.7% slower; Figure 1e). At 7 dph, larvae exposed to 0.08% and 0.2% slick oil exhibited an OMR at 1.1 and 1.5 rpm (revolutions per minute), respectively, which was significantly slower than control larvae (3.8 rpm; Figure 1e). By 10 dph, oil-exposed larvae increased their OMR by 7-fold from 7 dph, though it still exhibited a significantly reduced speed compared to control larvae (Figure 1e).

Transcriptome of Larval Mahi-Mahi Assembled by Trinity. Due to the lack of a reference genome for mahi-mahi, the transcriptome was *de novo* assembled with Trinity. Over 50 million Illumina HiSeq reads were generated from each pooled larval sample. After trimming the adapters, 170 183 689 bases were assembled, resulting in 258 722 transcript contigs with an average length of 658 bp and an N50 of 967 bases. 17 370 HMMER/PFAM protein domains (Pfam), 31 432 nonsuper-

DOI: 10.1021/acs.est.8b04169
Environ. Sci. Technol. 2018, 52, 13501−13510

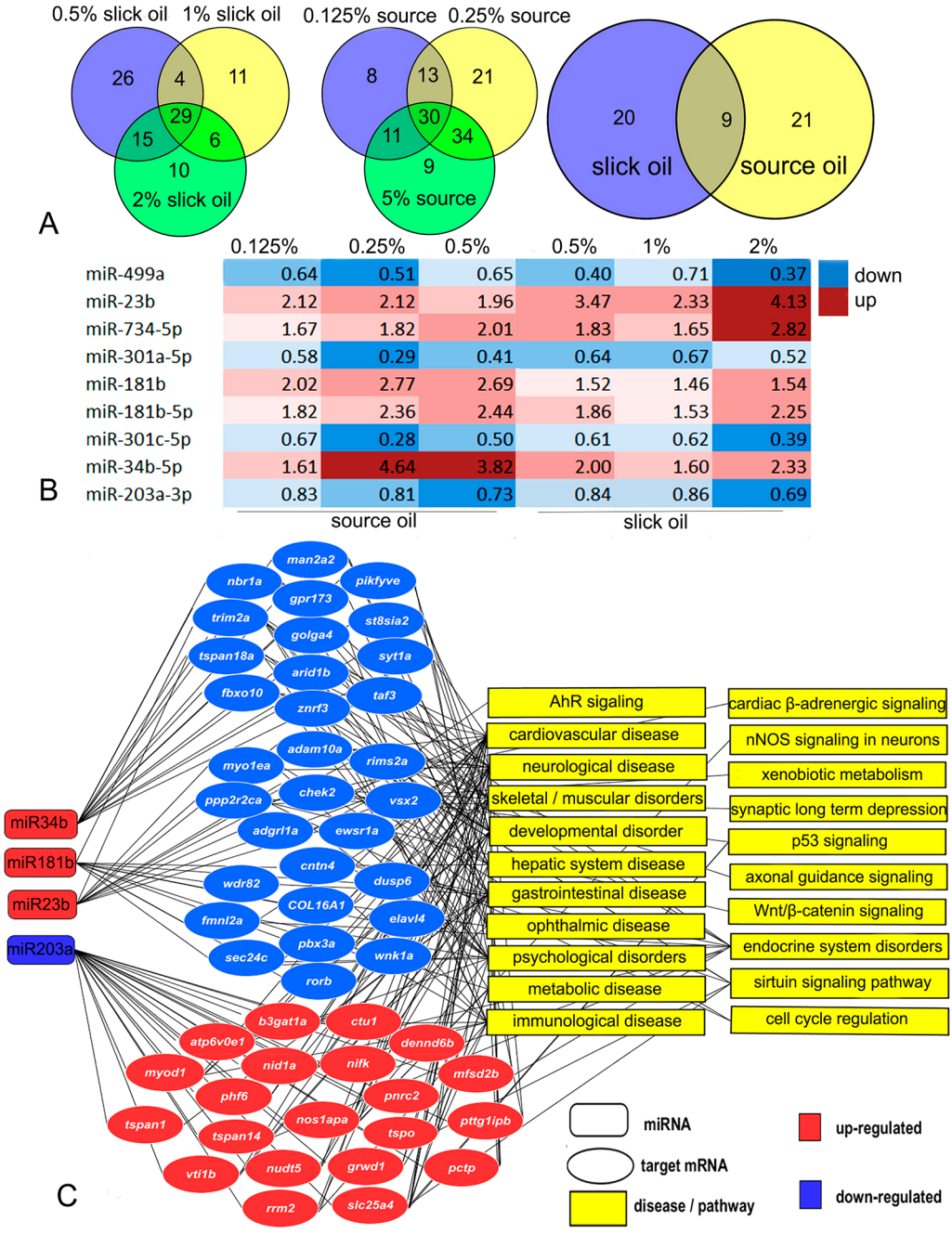

Figure 3. Venn diagrams of shared differentially expressed miRNA at the three different concentrations of slick and source oil exposure (A). Nine shared differentially expressed miRNA between slick and source oil exposure (B). Interaction networks of DE miRNAs identified potential DEGs involved in important signaling pathways and diseases by using the tool microRNA Target Filter of Ingenuity Pathway Analyses (C).

vised orthologous groups of genes (eggNOG), 34 847 GO_blast, and 18 375 GO_pfam were determined using Trinotate pipeline (Table S3). The final transcriptome assembly provided a high-quality template for further global gene differential expression analysis in this study.

Global Profiles of Differentially Expressed Genes (DEGs) and microRNAs (DE miRNAs). Overall, the unexposed control samples clustered separately from the slick or source oil treated samples, indicating global transcriptomic differences between the treatments (Figure S4). The numbers of DEGs were 540, 419, and 1304 with 0.5%, 1%, and 2% slick oil exposure, respectively (Figure 2). After 0.125%, 0.25%, and 0.5% source oil exposure, 1106, 1392, and 320 genes were significantly differentially expressed at FDR < 0.01, respectively. As for DE miRNAs, the numbers were 74, 50, and 60 after 0.5%, 1%, and 2% slick oil exposure, respectively (Figure 3a). Exposure to 0.125%, 0.25%, and 0.5% source oil resulted in 62, 98, and 84 altered miRNAs, respectively. Among different concentrations of slick and source oil exposure, 29 and 30 common DE miRNAs were identified, respectively (Figure 3a). Nine miRNAs were consistently up- (e.g., miR-23b, miR-181b, mi-34b-5p) or down-regulated (e.g., miR-203a-3p) at all exposure conditions, with dose-dependent fold changes (Figure 3b).

Biological Processes Affected by Slick and Source Oil Exposure. To determine the potential biological impact of oil exposure at a systematic level, a gene ontology (GO) term

DOI: 10.1021/acs.est.8b04169
Environ. Sci. Technol. 2018, 52, 13501−13510

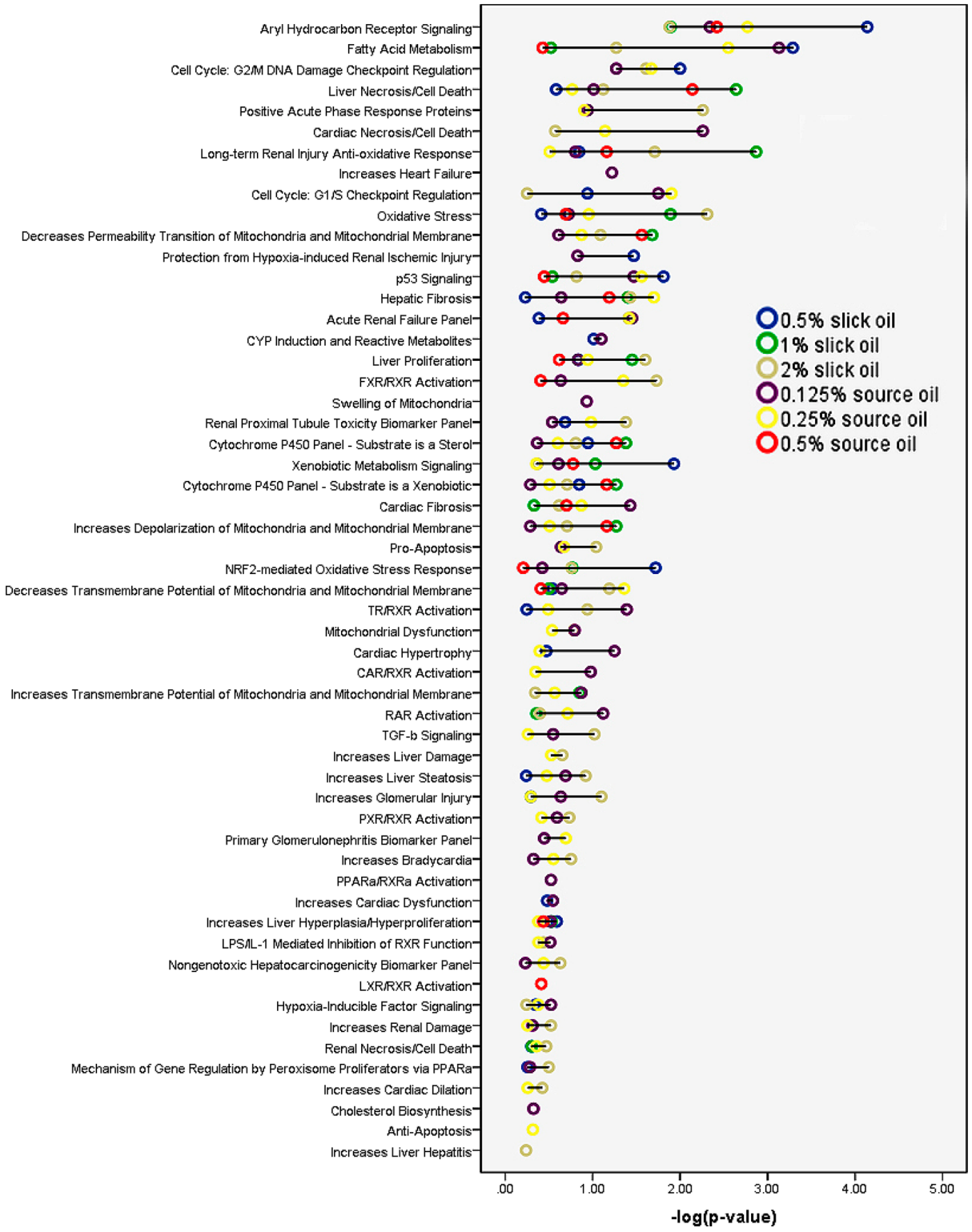

Figure 4. Toxicity Lists for slick and source oil predicted by Ingenuity Pathway Analyses (IPA). The *x*-axis displays the -log of *p*-value which is calculated by Fisher's exact test right-tailed. The *p*-value for a given biological process/pathway annotation is calculated by considering the number of focus genes that participate in that process/pathway as well as the total number of genes that are known to be associated with that process/pathway in the IPA reference data set.

analysis on biological processes (BPs) was conducted by analyzing the DEGs using ToppGene (Table S4) and DAVID (Table S5). The profile of BPs was dose- and oil type- dependent (Figure 2). After exposure to 0.5% slick oil, the top enriched BPs were terms associated with RNA processing and RNA metabolism (blue in Figure 2a) by ToppGene. Metabolic process (e.g., aromatic amino acid) and terms associated with embryo development (e.g., tissue morphogenesis and muscle cell differentiation) were some of the most enriched BPs after exposure to the 1% slick oil (Figure 2b). The top enriched BPs

DOI: 10.1021/acs.est.8b04169
Environ. Sci. Technol. 2018, 52, 13501−13510

for animals exposed to 2% slick oil were cellular catabolism and cardiovascular system development (green in Figure 2c). For source oil, cell cycle processes, metabolic processes, and RNA processing were the most enriched BPs after treatment with the 0.125% source oil exposure (Figure 2d). Similar processes were also highly enriched by 0.25% source oil exposure, while more "response" BPs were enriched by 0.25% source oil exposure, such as regulation of response to stress (Figure 2e). The most significantly enriched BP in animals by the 0.5% source oil was cardiovascular system development followed by cell junction assembly (Figure 2f). Consistent with BP profiles predicted by ToppGene, DAVID also predicted regulation of transcription, heart development, and cell proliferation as the top enriched terms for both oil types, with more embryonic and system development BPs at higher concentrations (Table S5).

Toxicity Pathways Identified Using IPA. Canonical pathways and toxicity lists in mahi-mahi larvae after slick and source oil exposure were analyzed by Ingenuity Pathway Analyses (IPA). The representative activated canonical pathways included EIF2 signaling, intrinsic prothrombin activation pathway, integrin signaling, signaling by RhoA family GTPases, cardiac β-adrenergic signaling, NRF2-mediated oxidative stress responses, and apoptosis pathways. Representative suppressed canonical pathways included Huntington's disease signaling, Gαq signaling, eNOS signaling, CREB signaling in neurons, and synaptic long-term potentiation pathways (Figure S5, Table S6). Notably, a number of significantly enriched canonical pathways such as the aryl hydrocarbon receptor (AhR) pathway, calcium signaling, and nNOS signaling in neurons interacted with other canonical pathways, and the complexity of the pathway networks depended on the concentrations and types of oil (Figure S6). IPA pathways focusing on the assessment of toxicity were further evaluated. The common toxicity pathways are listed in Figure 4, and a full list of toxicity-pathways and DEGs induced by slick and source oil are provided in Figure S7, Tables S7 and S8. AhR signaling, fatty acid metabolism, cell cycle, liver necrosis/cell death, positive acute phase responses proteins, cardiac necrosis/cell death, long-term renal injury, increases heart failure, and oxidative stress were the most significantly predicted toxicity pathways (Figure 4).

Meta-Analysis of miRNA−mRNA Functional Networks. On the basis of differentially expressed (DE) miRNAs and mRNAs, the interaction of miRNA−mRNA and their downstream functional consequences were predicted by using the MicroRNA Target Filter in the IPA database. Among 101 and 126 significant DE miRNAs, we identified 31 and 51 DE miRNAs which were linked from previous studies in the literature and also inversely correlated with the targeted DE mRNAs after slick and source oil exposure, respectively (Tables S9 and S10). Of these, four miRNAs were expressed in mahi-mahi larvae treated with all oil concentrations (miR-34b, miR-181b, miR-23b, and miR-203a). Consistent with biological process analysis by ToppGene/DAVID and toxicity pathway analysis by IPA, the target genes of these four miRNAs were involved in AhR signaling, cardiac β-adrenergic signaling, nNOS signaling in neurons, xenobiotic metabolism signaling, p53 signaling, and cell cycle regulation. In addition, predicted disease outcomes included cardiovascular disease, neurological disease, developmental disorders, ophthalmic disease, and metabolic diseases (Figure 3c).

DISCUSSION

Crude oil and PAHs have been shown to cause cardiotoxicity and morphological impacts on the eye.[7,8,12−14,20,27,28] To our knowledge, this is the first study to utilize miRNA−mRNA interactions in larval fish responsive to a series of diluted concentrations of weathered and nonweathered DWH oils, and provide four dose-dependent miRNA biomarkers that may be used in a combined way in subsequent oil studies. miRNAs have an important role in regulating mRNA stability and translation, with potential contributions to PAH-derived toxicity. We related the expression of these miRNAs to their target mRNAs, and to morphological, physiological, and behavioral-level responses associated with cardiac and visually mediated effects following oil exposure. Of the 29 common slick and 30 source oil DE miRNAs, nine were consistently up- (miR-23b; miR-734−5p; mir-181b; miR-181b-5p; miR-34b-5p) or down-regulated (miR-499a; miR-301a-5p; miR-301c-5p; miR-203a-3p). These miRNAs are predominantly associated with cardiovascular, eye, and brain development.[29−32]

There was a significantly increased pericardial area and bradycardia in larvae exposed to slick oil relative to control. This response is consistent with what was observed previously in larval mahi-mahi, as weathered slick oil tends to induce a greater cardiotoxic effect than nonweathered source oil.[13] A similar finding was seen in 48 to 72 hpf larval red drum exposed to slick oil, with a significantly increased pericardial area following exposure.[14,33] These data paralleled results of other studies that noted a similar response in larval, pelagic fishes.[7,11] Though various craniofacial deformities are commonly observed following oil exposure in larval fish,[8,34,35] there were no differences in eye size between exposed and control larvae at 48 hpf, regardless of concentration or oil type, as has been previously seen by others in 48 to 60 hpf larval mahi-mahi.[11] As larvae develop, their eyes grow proportional to their length,[36] with subsequent increases in visual acuity. We found a similar response, regardless of oil-exposure, with a strong relationship between eye size and total body length in larvae from 7 to 10 dph. However, the morphometric and histological assessment may not fully assess the effect of oil-exposure on eye development, as processes involved in visual signaling pathways which are among the most impacted following oil exposure, may manifest effects in other ways. When larval zebrafish were observed for visually induced effects following benzo-a-pyrene (BaP) exposure, Huang et al. found that, regardless of exposure concentration, histological differences in retinal layers did not significantly differ from controls.[37] However, transcriptomic-level dysregulation of eye-associated genes was reported following BaP exposure. Similarly, reductions in morphometric and histological measures of retinal size were not observed in oil-exposed larval mahi-mahi, though transcriptomic-level effects related to vision and visual function were impacted. In contrast, when a visually mediated behavioral assay was used to determine visual function in 7 to 10 dph larvae, oil-exposed larvae exhibited a significantly reduced optomotor response compared to control. Unfortunately, it was not possible to assess vision or behavior in 48 hpf larvae, so it is unclear whether transcriptional effects noted at 48 hpf are directly related to morphological effects at later stages, or whether animals exposed to oil at later stages are more susceptible to vision impairment. It has been postulated that the impairment of function at later stages is a result of altered blood flow due to cardiac toxicity.[38] The simultaneous change in expression of genes involved in vision

DOI: 10.1021/acs.est.8b04169
Environ. Sci. Technol. 2018, 52, 13501−13510

and cardiovascular function prior to morphological effects in the eye would suggest otherwise, but additional studies are needed to better understand the sequence of events following oil exposure.

To further assess the interaction among miRNA−mRNA and their associated functions, four commonly differentially expressed miRNAs (miR-34b, miR-181b, miR-23b, and miR-203a) were analyzed to predict downstream biological functions. The four miRNAs identified were involved in multiple biological processes and pathways predicted IPA. MiR-23b is associated with vascular and muscle development in zebrafish and blunt snout bream (*Megalobrama amblycephala*).[30,39] MiR-34b regulates kidney morphogenesis and olfactory organ development in zebrafish,[40] where it also plays a role in neuronal brain cell and heart development.[41,42] MiR-34b is positively regulated by the tumor suppressor transcription factor, p53, as a direct transcriptional target.[43] In the present study, p53 signaling was a major downstream biological pathway among the miRNAs consistently dysregulated following oil-exposure and this alteration could play a part in the upregulation of the upstream miR-34b. MiR-181b is predominately associated with visual function in the tectum and telencephalon in the brain and eyes in zebrafish,[16] particularly retinal ganglion cells, and inner nuclear layers.[44] The pretectal and tectal areas play an important role in visual function and processing as correct neuronal circuitry is dependent upon the upstream expression of miR-181.[44] Furthermore, the expression of miR-23b is involved in the activation, proliferation, and migration of endothelial cells in the eyes and heart in murine species,[45] where it plays an important role in vascular branching,[30] mediating proper capillary formation and choroidal neovascularization.[46] Downregulation of miR-203a was also observed after oil exposure and has been shown to upregulate *pax6b*, which increases the proliferation of progenitor cells associated with retinal regeneration in zebrafish.[47] Given that most of the miRNAs we found to be regulated in response to oil exposure in the whole larva are expressed in multiple organs and tissues, it will be of interest to determine whether these miRNAs regulate similar downstream biological effects of molecular toxicity pathways in specific organs or tissues. The tissue- and phenotype-specific miRNA expression profiles in fish are less understood in comparison with those in humans.[48] For example, of approximately 800 human miRNAs that have been identified, several have already been identified as potential biomarkers and clinical candidates in lung cancer (miR-203), colorectal cancer (miR-29a), heart disease (miR-208), neoangiogenesis (miR-33), and hepatitis C virus (miR-122)[49,50] In contrast to medical and clinical studies, the identification, profiling, and application of miRNAs in environmental studies especially oil studies is still in its infancy. To our knowledge, this study is the first to explore the global mRNA−miRNA signature post crude oil exposure. The four miRNAs identified here are dose-dependently expressed after crude oil exposure and strongly linked to specific phenotypes. Although the questions to how the crude oil initiates the dysregulation of miRNA expression are still unclear, some potential molecular mechanisms of action (MOA) may be implicated. PAHs in crude oil can regulate miRNA expression through induction of DNA methylation.[20] The transcription of miRNAs could also be altered by transcription factors that are dysregulated upon crude oil exposure. In addition, crude oil could affect the miRNA biogenesis pathway. These mechanisms may operate individually or in a combined way, which requires further investigations.

In summary, this study revealed miRNA−mRNA interactions associated with developmental impairments following treatment with DWH oil. Meta-analysis at the global transcriptomic-level identified molecular toxicity pathways that agreed with observed morphological, physiological, and behavioral-level impairments in larval fish exposed to different, environmentally relevant, doses of both source and weathered slick oil, suggesting that miRNAs may play an important role in the developmental toxicity of oil. The results of this study suggest specific DE miRNAs may be used as novel biomarkers of impaired brain, heart or vision in animals exposed to oil.

■ ASSOCIATED CONTENT

Supporting Information

The Supporting Information is available free of charge on the ACS Publications website at DOI: 10.1021/acs.est.8b04169.

Further information is available that provides a flowchart of experimental design (Figure S1), the assessments on eyes (Figures S2 and S3), heatmap showing the Euclidean distances between the control and oil-treated samples (Figure S4), disrupted canonical pathways (Figures S5 and S6; Table S6), Ingenuity Toxicity Lists (Figure S7; Tables S7 and S8), water quality measurements (Table S1), PAH measurements (Table S2), statistics of *de novo* transcriptome assembly (Table S3), top impacted biopathways (Tables S4 and S5), and list of differentially expressed miRNA and inversely correlated genes (Tables S9 and S10) (PDF)

■ AUTHOR INFORMATION

Corresponding Authors

*Phone: 1- 951-827-2018; fax: 1-951-827-3993; e-mail: genbo.xu@mail.mcgill.ca (E.G.X.)

*Phone: 1- 951-827-2018; fax: 1-951-827-3993; e-mail: dschlenk@ucr.edu (D.S.).

ORCID

Elvis Genbo Xu: 0000-0002-4414-1978

Present Address

‖Department of Chemical Engineering, McGill University, Montreal, QC H3A 0C5.

Notes

The authors declare no competing financial interest.

■ ACKNOWLEDGMENTS

This research was made possible by a grant from The Gulf of Mexico Research Initiative. Grant No: SA-1520; Name: Relationship of Effects of Cardiac Outcomes in fish for Validation of Ecological Risk (RECOVER). M.G. holds a Maytag Chair of Ichthyology. Data are publicly available through the Gulf of Mexico Research Initiative Information & Data Cooperative (GRIIDC). GRIIDC DOI: 10.7266/N7N29VHG.

■ REFERENCES

(1) Beyer, J.; Trannum, H. C.; Bakke, T.; Hodson, P. V.; Collier, T. K. Environmental effects of the Deepwater Horizon oil spill: a review. *Mar. Pollut. Bull.* **2016**, *110* (1), 28−51.

(2) Teo, S. L.; Block, B. A. Comparative influence of ocean conditions on yellowfin and Atlantic bluefin tuna catch from longlines in the Gulf of Mexico. *PLoS One* **2010**, *5* (5), e10756.

(3) Muhling, B. A.; Roffer, M. A.; Lamkin, J. T.; Ingram, G. W.; Upton, M. A.; Gawlikowski, G.; Muller-Karger, F.; Habtes, S.; Richards, W. J.

Overlap between Atlantic bluefin tuna spawning grounds and observed Deepwater Horizon surface oil in the northern Gulf of Mexico. *Mar. Pollut. Bull.* **2012**, *64*, 679−687.
(4) Rooker, J. R.; Kitchens, L. L.; Dance, M. A.; Wells, R. J. D.; Falterman, B.; Cornic, M. Spatial, temporal, and habitat-related variation in abundance of pelagic fishes in the Gulf of Mexico: potential implications of the Deepwater Horizon Oil Spill. *PLoS One* **2013**, *8*, e76080.
(5) Diercks, A. R.; Highsmith, R. C.; Asper, V. L.; Joung, D.; Zhou, Z.; Guo, L.; Shiller, A. M.; Joye, S. B.; Teske, A. P.; Guinasso, N.; Wade, T. L.; Lohrenz, S. E. Characterization of subsurface polycyclic aromatic hydrocarbons at the Deepwater Horizon site. *Geophys. Res. Lett.* **2010**, *37*, 1−6.
(6) Anon, N. D. Deepwater Horizon Natural Resource Damage Assessment Trustees. *Deepwater Horizon oil spill: Final Programmatic Damage Assessment and Restoration Plan and Final Programmatic Environmental Impact Statement*. 2016. Retrieved from http://www.gulfspill.
(7) Esbaugh, A. J.; Mager, E. M.; Stieglitz, J. D.; Hoenig, R.; Brown, T. L.; French, B. L.; Linbo, T. L.; Lay, C.; Forth, H.; Scholz, N. L.; Incardona, J. P.; Morris, J. M.; Benetti, D. D.; Grosell, M. The effects of weathering and chemical dispersion on Deepwater Horizon crude oil toxicity to mahi-mahi (*Coryphaena hippurus*) early life stages. *Sci. Total Environ.* **2016**, *543*, 644−651.
(8) Incardona, J. P.; Gardner, L. D.; Linbo, T. L.; Brown, T. L.; Esbaugh, A. J.; Mager, E. M.; Stieglitz, J. D.; French, B. L.; Labenia, J. S.; Laetz, C. A.; Tagal, M.; Sloan, C. A.; Elizur, A.; Benetti, D. D.; Grosell, M.; Block, B. A.; Scholz, N. L. Deepwater Horizon crude oil impacts the developing hearts of large predatory pelagic fish. *Proc. Natl. Acad. Sci. U. S. A.* **2014**, *111*, E1510−E1518.
(9) Mager, E. M.; Pasparakis, C.; Schlenker, L. S.; Yao, Z.; Bodinier, C.; Stieglitz, J. D.; Hoenig, R.; Morris, J. M.; Benetti, D. D.; Grosell, M. Assessment of early life stage mahi-mahi windows of sensitivity during acute exposures to *Deepwater Horizon* crude oil. *Environ. Toxicol. Chem.* **2017**, *36*, 1887−1895.
(10) Stieglitz, J. D.; Mager, E. M.; Hoenig, R. H.; Alloy, M.; Esbaugh, A. J.; Bodinier, C.; Benetti, D. D.; Roberts, A. P.; Grosell, M. A novel system for embryo-larval toxicity testing of pelagic fish: Applications for impact assessment of Deepwater Horizon crude oil. *Chemosphere* **2016**, *162*, 261−268.
(11) Edmunds, R. C.; Gill, J. A.; Baldwin, D. H.; Linbo, T. L.; French, B. L.; Brown, T. L.; Esbaugh, A. J.; Mager, E. M.; Stieglitz, J.; Hoenig, R.; Benetti, D.; Grosell, M.; Scholz, N. L.; Incardona, J. P. Corresponding morphological and molecular indicators of crude oil toxicity to the developing hearts of mahi-mahi. *Sci. Rep.* **2015**, *5*, 1−18.
(12) Mager, E. M.; Esbaugh, A. J.; Stieglitz, J. D.; Hoenig, R.; Bodinier, C.; Incardona, J. P.; Scholz, N. L.; Benetti, D. D.; Grosell, M. Acute embryonic or juvenile exposure to deepwater horizon crude oil impairs the swimming performance of mahi-mahi (*Coryphaena hippurus*). *Environ. Sci. Technol.* **2014**, *48*, 7053−7061.
(13) Xu, E. G.; Mager, E. M.; Grosell, M.; Pasparakis, C.; Schlenker, L. S.; Stieglitz, J. D.; Benetti, D.; Hazard, E. S.; Courtney, S. M.; Diamante, G.; Freitas, J.; Hardiman, G.; Schlenk, D. Time- and oil-dependent transcriptomic and physiological responses to Deepwater Horizon Oil in mahi-mahi (*Coryphaena hippurus*) embryos and larvae. *Environ. Sci. Technol.* **2016**, *50*, 7842−7851.
(14) Xu, E. G.; Khursigara, A. J.; Magnuson, J.; Hazard, E. S.; Hardiman, G.; Esbaugh, A. J.; Roberts, A. P.; Schlenk, D. Larval red drum (*Sciaenops ocellatus*) sublethal exposure to weathered Deepwater Horizon crude oil: Developmental and transcriptomic consequences. *Environ. Sci. Technol.* **2017**, *51*, 10162−10172.
(15) Kim, V. N. MicroRNA biogenesis: coordinated cropping and dicing. *Nat. Rev. Mol. Cell Biol.* **2005**, *6* (5), 376.
(16) Wienholds, E.; Kloosterman, W. P.; Miska, E.; Alvarez-Saavedra, E. MicroRNA expression in zebrafish embryonic development. *Science* **2005**, *309*, 310−311.
(17) Shkumatava, A.; Stark, A.; Sive, H.; Bartel, D. P. Coherent but overlapping expression of microRNAs and their targets during vertebrate development. *Genes Dev.* **2009**, *23* (4), 466−481.
(18) Lema, C.; Cunningham, M. J. MicroRNAs and their implications in toxicological research. *Toxicol. Lett.* **2010**, *198* (2), 100−105.
(19) Liu, N.; Olson, E. N. MicroRNA regulatory networks in cardiovascular development. *Dev. Cell* **2010**, *18* (4), 510−525.
(20) Huang, L.; Xi, Z.; Wang, C.; Zhang, Y.; Yang, Z.; Zhang, S.; Chen, Y.; Zuo, Z. Phenanthrene exposure induces cardiac hypertrophy via reducing miR-133a expression by DNA methylation. *Sci. Rep.* **2016**, *6*, 20105.
(21) Bianchi, M.; Renzini, A.; Adamo, S.; Moresi, V. Coordinated actions of microRNAs with other epigenetic factors regulate skeletal muscle development and adaptation. *Int. J. Mol. Sci.* **2017**, *18*, 840.
(22) Diamante, G.; Xu, E. G.; Chen, S.; Mager, E.; Grosell, M.; Schlenk, D. Differential expression of microRNAs in embryos and larvae of Mahi-Mahi (*Coryphaena hippurus*) exposed to Deepwater Horizon Oil. *Environ. Sci. Technol. Lett.* **2017**, *4*, 523−529.
(23) Goodson, J. M.; Weldy, C. S.; Macdonald, J. W.; Liu, Y.; Bammler, T. K.; Chien, W.; Chin, M. T. In utero exposure to diesel exhaust particulates is associated with an altered cardiac transcriptional response to transverse aortic constriction and altered DNA methylation. *FASEB J.* **2017**, *31*, 4935−4945.
(24) Xu, E. G.; Mager, E. M.; Grosell, M.; Stieglitz, J. D.; Hazard, E. S.; Hardiman, G.; Schlenk, D. Developmental transcriptomic analyses for mechanistic insights into critical pathways involved in embryogenesis of pelagic mahi-mahi (*Coryphaena hippurus*). *PLoS One* **2017**, *12* (7), e0180454.
(25) Stieglitz, J. D.; Hoenig, R. H.; Kloeblen, S.; Tudela, C. E.; Grosell, M.; Benetti, D. D. Capture, transport, prophylaxis, acclimation, and continuous spawning of Mahi-mahi (*Coryphaena hippurus*) in captivity. *Aquaculture* **2017**, *479*, 1−6.
(26) Xu, E. G.; Mager, E. M.; Grosell, M.; Hazard, E. S.; Hardiman, G.; Schlenk, D. Novel transcriptome assembly and comparative toxicity pathway analysis in mahi-mahi (*Coryphaena hippurus*) embryos and larvae exposed to Deepwater Horizon oil. *Sci. Rep.* **2017**, *7*, 44546.
(27) Huang, L.; Wang, C.; Zhang, Y.; Wu, M.; Zuo, Z. Phenanthrene causes ocular developmental toxicity in zebrafish embryos and the possible mechanisms involved. *J. Hazard. Mater.* **2013**, *261*, 172−180.
(28) Incardona, J. P.; Scholz, N. L. The influence of heart developmental anatomy on cardiotoxicity-based adverse outcome pathways in fish. *Aquat. Toxicol.* **2016**, *177*, 515−525.
(29) Wilson, K. D.; Hu, S.; Venkatasubrahmanyam, S.; Fu, J. D.; Sun, N.; Abilez, O. J.; Baugh, J. J.; Jia, F.; Ghosh, Z.; Li, R. A.; Butte, A. J.; Wu, J. C. Dynamic microRNA expression programs during cardiac differentiation of human embryonic stem cells: role for miR-499. *Circ.: Cardiovasc. Genet.* **2010**, *3* (5), 426.
(30) Biyashev, D.; Veliceasa, D.; Topczewski, J.; Topczewska, J. M.; Mizgirev, I.; Vinokour, E.; Reddi, A. L.; Licht, J. D.; Revskoy, S. Y.; Volpert, O. V. miR-27b controls venous specification and tip cell fate. *Blood* **2012**, *119*, 2679−2688.
(31) Wu, J.; Bao, J.; Kim, M.; Yuan, S.; Tang, C.; Zheng, H.; Mastick, G. S.; Xu, C.; Yan, W. Two miRNA clusters, miR-34b/c and miR-449, are essential for normal brain development, motile ciliogenesis, and spermatogenesis. *Proc. Natl. Acad. Sci. U. S. A.* **2014**, *111*, E2851.
(32) Bhattacharya, M.; Sharma, A. R.; Sharma, G.; Patra, B. C.; Nam, J.; Chakraborty, C.; Lee, S.-S. The crucial role and regulations of miRNAs in zebrafish development. *Protoplasma* **2017**, *254*, 17−31.
(33) Khursigara, A. J.; Perrichon, P.; Bautista, N. M.; Burggren, W. W.; Esbaugh, A. J. Cardiac function and survival are affected by crude oil in larval red drum, *Sciaenops ocellatus*. *Sci. Total Environ.* **2017**, *579*, 797−804.
(34) Hose, J. E.; McGurk, M. D.; Marty, G. D.; Hinton, D. E.; Brown, E. D.; Baker, T. T. Sublethal effects of the Exxon Valdez oil spill on herring embryos and larvae: morphological, cytogenetic, and histopathological assessments, 1989−1991. *Can. J. Fish. Aquat. Sci.* **1996**, *53*, 2355−2365.
(35) Sørhus, E.; Incardona, J. P.; Karlsen, Ø.; Linbo, T.; Sørensen, L.; Nordtug, T.; Van Der Meeren, T.; Thorsen, A.; Thorbjørnsen, M.; Jentoft, S.; Edvardsen, R. B.; Meier, S. Crude oil exposures reveal roles for intracellular calcium cycling in haddock craniofacial and cardiac development. *Sci. Rep.* **2016**, *6*, 31058.

DOI: 10.1021/acs.est.8b04169
Environ. Sci. Technol. 2018, 52, 13501−13510

(36) Blaxter, J. H. S.; Jones, M. P. The development of the retina and retinomotor responses in the herring. *J. Mar. Biol. Assoc. U. K.* **1967**, *47*, 677−697.
(37) Huang, L.; Zuo, Z.; Zhang, Y.; Wu, M.; Lin, J. J.; Wang, C. Use of toxicogenomics to predict the potential toxic effect of Benzo(a)pyrene on zebrafish embryos: Ocular developmental toxicity. *Chemosphere* **2014**, *108*, 55−61.
(38) Incardona, J. P.; Carls, M. G.; Holland, L.; Linbo, T. L.; Baldwin, D. H.; Myers, M. S.; Peck, K. A.; Tagal, M.; Rice, S. D.; Scholz, N. L. Very low embryonic crude oil exposures cause lasting cardiac defects in salmon and herring. *Sci. Rep.* **2015**, *5*, 1−13.
(39) Yi, S.; Gao, Z. X.; Zhao, H.; Zeng, C.; Luo, W.; Chen, B.; Wang, W. M. Identification and characterization of microRNAs involved in growth of blunt snout bream (*Megalobrama amblycephala*) by Solexa sequencing. *BMC Genomics* **2013**, *14* (1), 754.
(40) Wang, L.; Fu, C.; Fan, H.; Du, T.; Dong, M.; Chen, Y.; Jin, Y.; Zhou, Y.; Deng, M.; Gu, A.; Jing, Q.; Liu, T.; Zhou, Y. miR-34b regulates multiciliogenesis during organ formation in zebrafish. *Development* **2013**, *140*, 2755−2764.
(41) Kapsimali, M.; Kloosterman, W. P.; de Bruijn, E.; Rosa, F.; Plasterk, R. H. A.; Wilson, S. W. MicroRNAs show a wide diversity of expression profiles in the developing and mature central nervous system. *Genome Biol.* **2007**, *8*, R173.
(42) Bernardo, B. C.; Gao, X. M.; Winbanks, C. E.; Boey, E. J.; Tham, Y. K.; Kiriazis, H.; Gregorevic, P.; Obad, S.; Kauppinen, S.; Du, X. J.; Lin, R. C.; McMullen, J. R. Therapeutic inhibition of the miR-34 family attenuates pathological cardiac remodeling and improves heart function. *Proc. Natl. Acad. Sci. U. S. A.* **2012**, *109* (43), 17615−17620.
(43) Bommer, G. T.; Gerin, I.; Feng, Y.; Kaczorowski, A. J.; Kuick, R.; Love, R. E.; Zhai, Y.; Giordano, T. J.; Qin, Z. S.; Moore, B. B.; MacDougald, O. A.; Cho, K. R.; Fearon, E. R. p53-mediated activation of miRNA34 candidate tumor-suppressor genes. *Curr. Biol.* **2007**, *17*, 1298−1307.
(44) Carrella, S.; D'Agostino, Y.; Barbato, S.; Huber-Reggi, S. P.; Salierno, F. G.; Manfredi, A.; Neuhauss, S. C. F.; Banfi, S.; Conte, I. miR-181a/b control the assembly of visual circuitry by regulating retinal axon specification and growth. *Dev. Neurobiol.* **2015**, *75*, 1252−1267.
(45) Zhou, Q.; Gallagher, R.; Ufret-Vincenty, R.; Li, X.; Olson, E. N.; Wang, S. Regulation of angiogenesis and choroidal neovascularization by members of microRNA-23 ~ 27 ~ 24 clusters. *Proc. Natl. Acad. Sci. U. S. A.* **2011**, *108*, 8287−8292.
(46) Agrawal, S.; Chaqour, B. MicroRNA signature and function in retinal neovascularization. *World J. Biol. Chem.* **2014**, *5*, 1−11.
(47) Rajaram, K.; Harding, R. L.; Hyde, D. R.; Patton, J. G. miR-203 regulates progenitor cell proliferation during adult zebra fi sh retina regeneration. *Dev. Biol.* **2014**, *392*, 393−403.
(48) Bizuayehu, T. T.; Babiak, I. MicroRNA in teleost fish. *Genome Biol. Evol.* **2014**, *6* (8), 1911−1937.
(49) Reid, G.; Kirschner, M. B.; van Zandwijk, N. Circulating microRNAs: Association with disease and potential use as biomarkers. *Crit. Rev. Oncol. Hematol.* **2011**, *80* (2), 193−208.
(50) van Rooij, E.; Purcell, A. L.; Levin, A. A. Developing microRNA therapeutics. *Circ. Res.* **2012**, *110* (3), 496−507.

DOI: 10.1021/acs.est.8b04169
Environ. Sci. Technol. 2018, 52, 13501−13510